Analyse of Flux Density and Iron Loss Distributions in Segmented Magnetic Circuits Made with Mixed Electrical Steel Grades

A. Rebhaoui, Sidi-Ali Randi, C. Demian, J-Ph. Lecointe

Analyse of Flux Density and Iron Loss Distributions in Segmented Magnetic Circuits Made with Mixed Electrical Steel Grades

A. Rebhaoui[1,2], S.A. Randi[2,3], C. Demian[1], J-Ph. Lecointe[1]

[1] Univ. Artois, UR 4025, Laboratoire Systèmes Electrotechniques and Environnement (LSEE), Béthune, F-62400, France
[2] Institut VEDECOM, 78000 Versailles, France
[3] Technocentre RENAULT, 78288 Guyancourt, France

This paper presents the potential contribution of segmented stator magnetic circuits of rotating permanent magnets electrical machines with concentric winding. Two magnetic materials are mixed, FeSi Non-Oriented Electrical Steel (NOES) and FeSi Grain Oriented Electrical Steel (GOES). The choice of using GOES is based on the high performance it offers in terms of permeability and iron losses compared to conventional NOES, particularly when GOES is magnetised in the Rolling Direction (RD). The goal is to analyse the contribution of the mixed magnetic circuit on the losses and electromagnetic torque, but also the drawbacks due to the cut process and to the assembly. The behaviour of the magnetic field at the junction between the segments is studied by comparing different geometrical connection shapes and compared to a reference magnetic circuit fully made with NOES sheets. This comparison is experimentally made with a model representative of the existing phenomena in an electrical machine. In addition, numerical calculations using finite elements software are carried out, by considering both the magnetic anisotropy and the saturation of the GOES.

***Keywords*– Electrical machines, Grain oriented electric steel, Iron losses Magnetic circuit, Mixed electrical steels.**

I. Introduction

The global warming constitutes one of the biggest environmental problems, caused by the Greenhouse Gas (GhG) emissions, especially the CO2 [1]. As road transports are often considered the main source of GhG in many countries, the European commission and regulations increase the CO2 emission limits. Car manufacturers who fail to reach these limits face significant financial penalties in Europe [1]. As a result, the need for performant electric vehicles increases. On the other hand, the limited battery autonomy of electric vehicles is still a constraint for consumers. Moreover, to become widely accepted by society, hybrid electric vehicles (HEV) and full battery electric vehicle (BEV) must be efficient [1]. That explains why reducing the rate of CO2 emissions for HEV and improving the autonomy for BEV constitute a major challenge for motor manufacturers [1]. It can be done by reducing the losses of each part of the electric powertrains. Concerning the electric motors, there are many trends in their development to improve their efficiency [2]. Among them, using high grade magnetic materials and optimizing their design allow to reduce iron losses for loads in the torque-speed plane [3].

Conventionally, the stator and rotor magnetic circuits are made of Non-Oriented Grain Electrical Steel (NOES) laminations [2]. The Grain Oriented Electrical Steel (GOES) is usually used in the manufacture of power transformers [3]. The field direction is mainly unidirectional, which is well adapted to exploit the GOES properties of the Rolling Direction (RD) [4]. The GOES moderate cost and the low iron losses in the RD when compared with NOES make this material an attractive candidate to improve efficiency of eMotors used in automotive applications [5]. That is why segmented stator cores mixing GOES and NOES constitute a serious way of improvement.

The aim of this work is to quantify the contribution and the potential benefit of using a high-grade magnetic material in concentric winding permanent magnets electric motors, with the goal of improving performances and reducing iron losses. The technique consists in replacing the stator teeth by GOES teeth fixed on a NOES yoke. The study is focused on two important points:

- the sensitivity of the magnetic sheets to cutting stresses;
- the behaviour of the magnetic field lines at the tooth-yoke junction, between the two materials.

The paper is divided into 4 principles parts. The first part presents the advantages and the constraints of GOES in electric motors, compared to conventional NOES sheets, in terms of permeability, iron losses, magnetic anisotropy and sensitivity to manufacturing processes. In addition, the modelling of magnetic anisotropy in finite element analysis software is presented. The second part presents a brief review of the electric motors using GOES magnetic circuits and their advantages compared to the classical motors. The third part presents a device for modelling the different junctions between the GOES teeth and the NOES yoke as in electric motors with concentric windings. Influence of the junction geometry is analysed with experimental measurements and FEA calculations. The fourth part analyses with FEA calculations the mixed motor performance compared to a full NOES reference motor in terms of electromagnetic torque, drag losses and iron losses.

II. Electrical steel sheets characteristics

A. *Magnetic properties*

The advantage of the GOES sheets when compared with NOES sheets is, from a macroscopic scale, shown by analysing the standardized measurements, in terms of permeability, saturation flux density level and iron losses.

Figure 1 shows the B-H curves of a 0.20mm thickness isotropic NOES sheet and a 0.20mm anisotropic GOES sheet, the latter being magnetised along the Rolling Direction (RD) and the Transverse Direction (TD). The measures are obtained with a standardized Single Sheet Tester (SST) at 50Hz, 500Hz and up to 1000Hz. The GOES saturation knee for RD occurs at a higher induction level, compared to the NOES sheet.

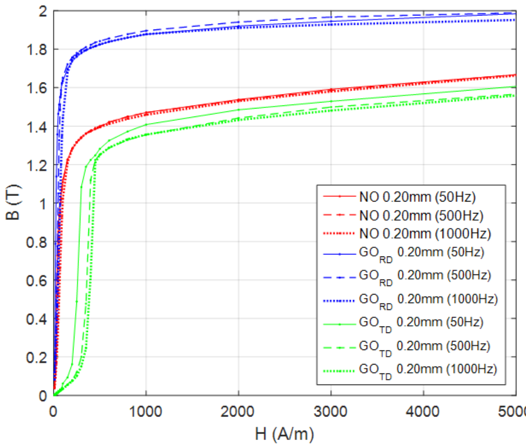

Fig. 1. B-H curves of NOES and GOES along the RD and TD at 50Hz

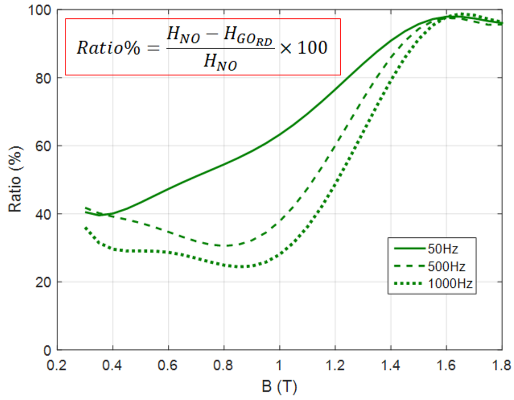

Fig. 2. Magnetic field reduction ratio with GOES along the RD compared to the reference NOES

At iso frequency and for a given flux density, the GOES sheet magnetised in the RD requires a lower magnetic field intensity, compared to the NOES sheet. This reduction ratio, at 50Hz, goes from 40% at 0.5T up to 97% at 1.7T (Fig. 2). That can also impact positively the Joule losses of electrical machines for a given flux density. This ratio decreases when the frequency increases. The GOES maximum permeability value is more reduced than NOES sheets, especially when magnetised in the TD (Fig. 1).

Figure 3 shows the specific loss curves as a function of flux density obtained with a standardized SST, for the NOES and GOES sheets previously mentioned, at 50Hz, 500Hz and 1000Hz. GOES sheets, magnetised along the RD, always have an advantage in terms of iron losses reduction, compared to NOES sheet. For example, at 50Hz, the average reduction is about 70% for GOES compared to NOES sheet of same thickness. However, this reduction ratio decreases for higher frequencies: at 1000Hz, the reduction ratio is 41% at 1.5T and 23% at 0.5T (Figure 4).

GOES has the disadvantage of being highly anisotropic, and the magnetic performance is not so interesting along the TD, compared to the NOES sheet, especially in terms of permeability and iron losses. For flux density values below 1.2T, the GOES sheet magnetised in the TD requires a magnetic field intensity more than 200% higher compared to

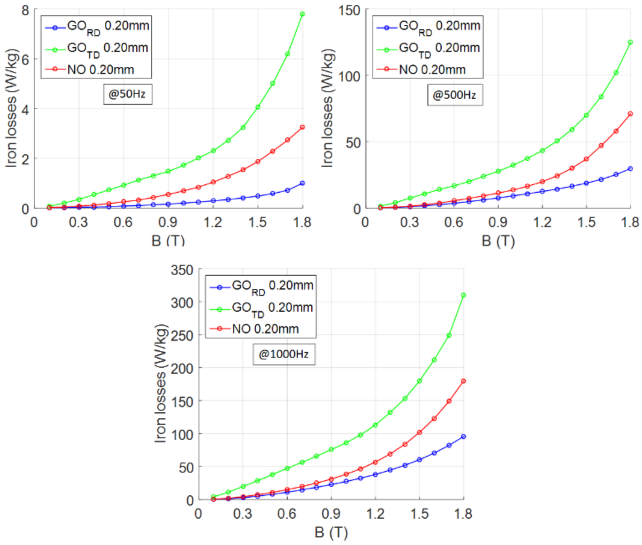

Fig. 3. Specific losses curve of NOES and GOES (along the RD and TD) at 50Hz, 500Hz and 1000Hz

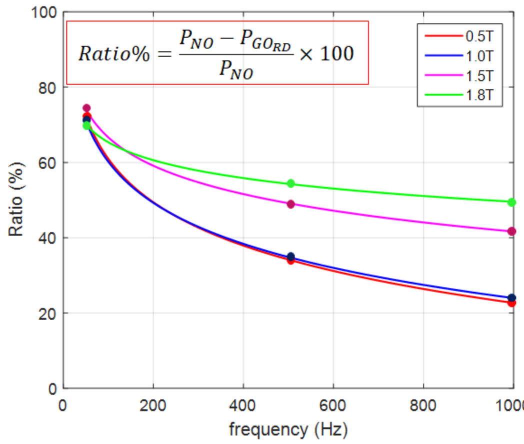

Fig. 4. Iron losses reduction ratio with GOES along the RD compared to the reference NOES

the NOES sheet. At a given flux density, the GOES iron losses are very high in the TD when compared to NOES. This iron loss ratio exceeds, on average, over 2, particularly at low flux density values.

B. *Effect of cutting on magnetic properties*

The iron losses in an electrical machine are systematically higher than the values given in the manufacturer catalogues. The causes of this degradation are the mechanical stresses due to the manufacturing, the pressure applied to the sheets when inserted and fixed in the external yoke and especially the effect of the cutting.

From a microscopic point of view, the cutting destroys the grains near the edges of the cut as an effect of plastic deformation and thermal impact [6] [7]. The GOES grains are much larger than NOES (Fig. 5); they can have centimetric dimensions (up to 5 cm) [8] making them particularly sensitive to the cutting. From a macroscopic scale, the cutting causes a significant degradation of the magnetic performances, depending not only on the cutting technique but also on the dimensions of the sheet [9]. To analyse the effect of cutting, the authors characterize four Epstein samples of standardized strips, shown in figure 6. The strips are cut several times along their length; the red lines represent the laser cut lines, which start at 1cm from the overlap region, to allow a better distribution of the magnetic flux around the

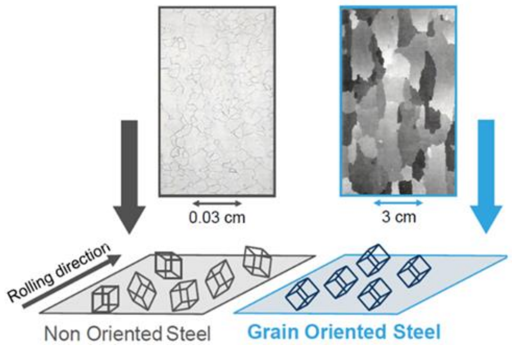

Fig. 5. Comparison of GOES and NOES sheet structures: grain sizes and crystalline networks orientation [8]

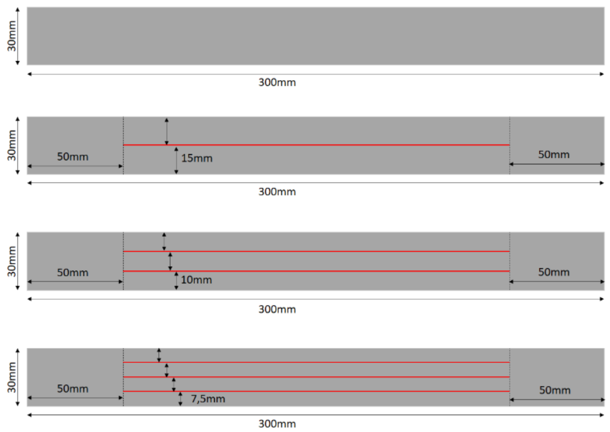

Fig. 6. Samples of standardised Epstein strips with 0, 1, 2, 3 slots

corners. That is why the strips are uncut 5cm from the extremities. This study is carried out for 0.20mm NOES and GOES sheets cut along the rolling direction (RD), by fibre laser cutting, whose parameters are presented in table I.

TABLE I
TECHNICAL SPECIFICATIONS OF THE LASER CUTTER

Manufacturer / Brand	Stiefelmayer Lasertechnik
Laser type	Fibre
Class / Standard	IEC 60825 – class 4
Power	1000 W
Output fibre	100 µm
Wavelength	1080 ± 10 nm

Standardized measurement results obtained with an Epstein frame are shown in Fig.7, with B-H curves and specific losses at 50Hz. It shows that the cutting of the strips deteriorates the magnetic performance of NOES and GOES in the RD with a decrease of the magnetic permeability and an increase of the iron losses.

In terms of magnetic permeability, the cutting causes an increase in the magnetic field strength required for a given flux density. For the NOES at 1.5T, 630A/m are required for the 3-slot strips, compared to 300A/m for the strips without slots, which means the degradation is over of 100%. In parallel, for the GOES at 1.5T, 85A/m are necessary for the 3-slot strips, against 40A/m for the structure without slots, corresponding to a degradation over 100%. This ratio is weakened by saturating the sheets and it is slightly impacted by the operating frequency. Despite the degradation, the GOES sheet magnetised along the RD has a better permeability than the NOES sheets.

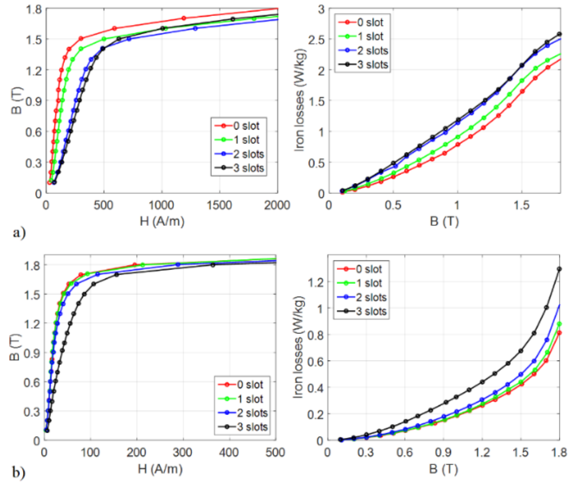

Fig. 7. Epstein measurements of magnetic performances, B-H curves and specific losses at 50Hz: a) NOES sheets, b) GOES sheets width)

The rate of iron loss degradation (compared to a standard strip without slots) is strongly impacted by the slotting, for both NOES and GOES sheets. As shown in Fig. 8, the strong degradation occurs for the highest number of slots in the strips which may be overly impacted by the thermal effect of the laser cutting at the cut edges. For NOES, strip cut every 0.75cm are degraded of 25% at 1.5T at 50Hz, compared to a 3cm NOES strip. For GOES, this degradation rate is very high for the smallest strip widths. It exceeds 60% for strips cut every 0.75cm compared to 3cm GOES strips.

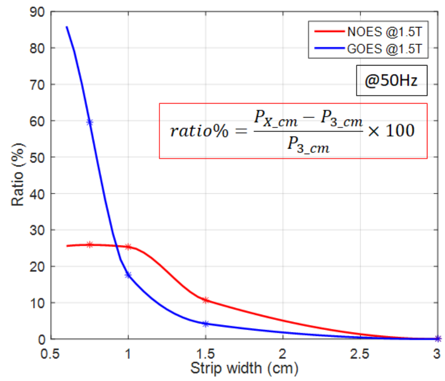

Fig. 8. Iron loss degradation ratio, at 50Hz, as a function of cut strip width compared to the standard Epstein strip

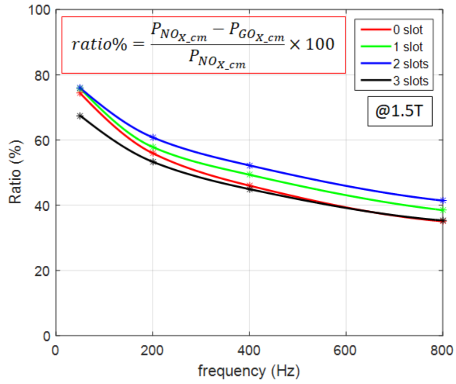

Fig. 9. Iron loss reduction ratio with GOES (along the RD) compared to NOES at iso strip width in function of frequency

Fig. 9 shows that the iron loss reduction rate is weakly impacted by the frequency: about 70%, at low frequency up to 40% at 800Hz. As explained previously, the grain sizes are large, implying a high sensitivity of the sheet to the cutting. Although the GOES has high iron losses degradation ratios in the RD and for low geometrical dimensions, it keeps better performances than the NOES, at iso-strip width.

C. FEA MODELLING OF ANISOTROPY

The modelling of electrical steel is still challenging for anisotropic GOES sheets, because of the magnetic characteristics that differ as a function of the magnetisation angle [10]. Several methods for modelling magnetic anisotropy exist [10] [11] [12] [13] [14] [15]. The Table II shows a synthetic view of the different magnetic anisotropy modelling techniques, considering the compromise of the magnetic performances and the state of the material knowledge.

TABLE II
MODELLING METHODS FOR MAGNETIC ANISOTROPY

Modelling method	knowledge of the material	Low flux density	High flux density	difficult magnetisation angle (55°/RD)
Two-axis anisotropic method **[11]**	**Poor** (main directions of magnetization)	+++	++	+
Elliptic model **[12]**	**Poor** (main directions of magnetization)	+++	+	+
Co-energy model **[15]**	**Poor** (main directions of magnetization)	++	+	+
Orientation distribution function (ODF) **[13]**	**Medium-Strong** (multiple directions of magnetization)	+	+++	++
Scalar model **[14]**	**Strong** (permeability in all directions)	++	+++	++
Reference model **[10]**	**Very strong** (permeability and magnetisation angle in all directions)	++++	++++	++++

Existing commercial Finite Element Analysis (FEA) software applications models anisotropy as a diagonal permeability tensor (the two-axis anisotropic method) based on measurements of the magnetic characteristics in the main directions, i.e. the RD and TD for 2D calculation. The permeability in the Normal Direction (ND) is added for 3D models [11].

$$B = \begin{bmatrix} \mu_x & 0 & 0 \\ 0 & \mu_y & 0 \\ 0 & 0 & \mu_z \end{bmatrix} \times H \quad (1)$$

For the two-axis method used in JMAG software application (version 19.1), a vector relationship is applied between the flux density B and the magnetic field H for each main direction to determine B and H in the intermediate directions (2). This software allows to consider both saturation and anisotropy of the magnetic circuit.

$$\begin{cases} B_x = B.\cos(\theta_B) \\ B_y = B.\sin(\theta_B) \end{cases}$$

$$\begin{cases} H_x = f_x(B_x) \\ H_y = f_y(B_y) \end{cases} \rightarrow \begin{cases} H = \sqrt{H_x^2 + H_y^2} \\ \theta_H = \tan^{-1}\left(\frac{H_y}{H_x}\right) \end{cases} \quad (2)$$

In commercial FEA software, the most popular methods for calculating iron losses are the Steinmetz model and the modified Steinmetz model (Bertotti model) [16]. In JMAG software application for anisotropic GOES sheets, the classical Steinmetz model approximation with bidirectional coefficients along the RD and TD is used, considering the harmonics presented in equation 3 where P_h is the hysteresis losses, P_e the eddy current losses, i the harmonic rank, N the highest considered harmonic and f the frequency. B_{RD} and B_{TD} are the maximum levels of flux density in the RD and the TD respectively. The coefficients $K_{h_{RD}}$, $K_{h_{TD}}$, $K_{e_{RD}}$, $K_{e_{TD}}$, α, β, γ and δ are determined with measurement data (iron loss curves as a function of flux density and frequency).

$$P_{core\_loss} = P_h + P_e = \sum_{i=1}^{N} \begin{cases} \left(K_{h_{RD}}.\ B_{RD}^{\alpha} + K_{h_{TD}}.\ B_{TD}^{\alpha}\right).f^{\beta} \\ + \\ \left(K_{e_{RD}}.\ B_{RD}^{\gamma} + K_{e_{TD}}.\ B_{TD}^{\gamma}\right).f^{\delta} \end{cases} \quad (3)$$

For the FEA simulations, the sheet steel data used for the estimation of the iron losses are shown in Table III. These data were obtained with normalized SST measurements without sheet annealing.

TABLE III.
IRON LOSSES DATA RANGE

	NOES	GOES
Flux density	[0.1 T – 1.82 T]	[0.1 T – 2.1 T]
Frequency	[50, 100, 200, 400, 500, 1000, 2000, 5000] Hz	[50, 100, 200, 400, 500, 1000, 2000, 5000] Hz

III. MAGNETIC CIRCUITS BASED ON GOES SHEETS IN ROTATING ELECTRICAL MACHINES

The strong anisotropy of GOES can be an obstacle to use this steel in rotating field electrical machines. Using GOES requires adapting the magnetic circuit to the specificities of the sheet to exploit it, as far as possible, in the RD to take advantage of the best performances.

Exploiting the optimal properties of GOES sheets leads to considerate the machine topology. Some yokeless axial flux structures are well adapted as in [17] and [18] which present a yokeless axial flux motor with two permanent magnet rotors (Fig.10). The central stator magnetic circuit has teeth made of GOES sheets, which allows the magnetic flux to be driven mainly in the RD. They show the use of GOES makes it possible to reduce the stator iron losses, at no load condition, by a ratio of 5 (at 267Hz). The electromagnetic torque is improved by 10% for the same rated current [17].

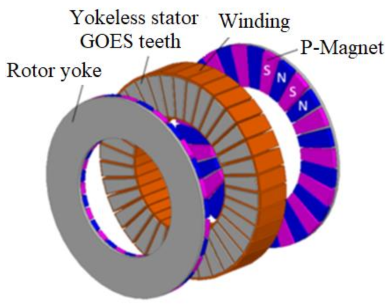

Fig. 10. Yokeless permanent magnet axial flux electric motors based on GOES teeth

Two techniques exist for radial structures of electrical machines based on GOES laminations:

- The segmentation of the magnetic circuit to place the RD along the direction of the field lines [5] [19];
- Spatial angular shifting of one piece GOES laminations to place the RD regularly all along the stator [20] [21].

Segmentation consists in attaching GOES teeth to the stator and/or rotor on a yoke, which can also be made of segmented GOES pieces. It can also be made by sectors with a part of the yoke and one or several teeth, as in large turbogenerators. [22] describes the first application of GOES segments in stators of large radial flux generators in 1951. The easy magnetisation direction of the sheets coincides with the direction of the magnetic field in the yoke or in the teeth being quite wide (Fig.11-a). For hydraulic generators, which are slow and therefore have many poles, the direction of easy magnetisation coincides with the radial direction of the teeth (Fig.11-b). The results of tests on 16 machines show a reduction of 25 to 30% in iron losses, as well as a 50% reduction in the value of the current for a given power, compared to machines with NO plates, with the same geometric dimensions.

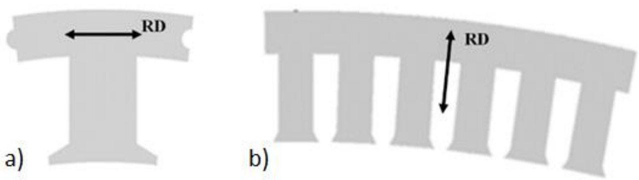

Fig. 11. Turbo-alternator magnetic circuit with GOES segments: a) RD in the yoke, b) RD along the teeth [22]

The technique of segmenting GOES in sectors is also presented in [23] with a radial permanent magnet (PM) motor. Each "T" sector has a tooth and a yoke portion, where the direction of easy magnetisation of the GOES sheet is parallel with the yoke field (Fig.11-a). Efficiency is improved by 3% at low power and low speed compared to a NOES motor. At high operating speeds, the iron losses for both motors become comparable.

In [24], a 48 GOES teeth PM synchronous motor (Fig. 12-a) is experimentally compared with a NOES reference motor. At iso-current, maximum electromagnetic torque is improved of 4.3% as well as the efficiency of more than 1.2% at low speed and of 2.7% at high speed. Switched reluctance motor (SRM) [19] (Fig. 12-b) has also been equipped of segmented GOES teeth in the stator and in the rotor. The efficiency is increased by more than 3 points at low speed compared to a NOES motor.

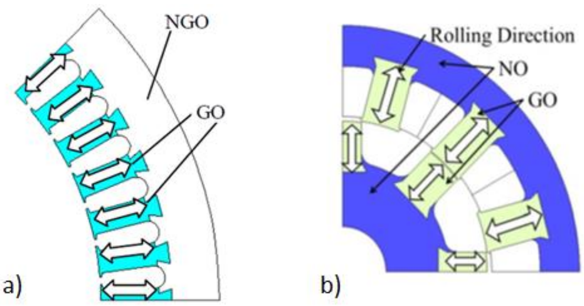

Fig. 12. Electric motors with GOES sheets teeth: a) in the stator, b) in the stator and rotor [24] [19]

[25] and [26] concern a 4-pole SRM with a multi-layer flux barrier in the rotor for an electric traction application. The rotor is made of 4 GOES segments whose RD is quasi-parallel to the conductive flux barriers. The prototype improves the saliency ratio by 47% and thus the torque-current characteristic compared to a conventional NOES rotor.

In [5] [27] [28], the authors have studied and realized a GOES

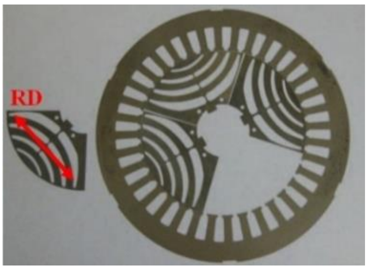

Fig. 13. SRM with GOES segmented rotor [26]

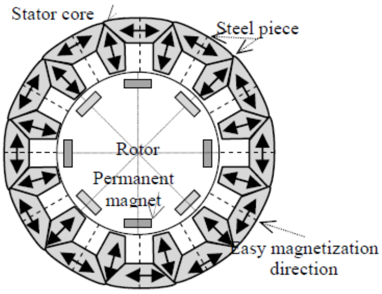

Fig. 14. Fully segmented GOES stator [5]

PM stator fully segmented, where the RD of the sheet is maintained in the direction of the field lines in the yoke and in the tooth (Fig.14). FEA simulations showed a 43% reduction in drag losses and a 2% improvement in torque at rated operation. Experimental results showed a lower loss reduction: 24% reduction in drag losses and 27% in core losses at 3000 rpm and no-load.

IV. Methodology Used for the Magnetic Analysis in a Segmented Magnetic Circuit

A. *Introduction of the studied motor (HEV eMotor)*

Several hybrid car manufacturers have developed Integrated Motor Assist technology with a fractionally wound concentric PMSM. Concentric winding allows to automate the manufacturing process. For example, the 24-slot (Q) 16-pole (P) structure leads to less acoustic noise and vibrations of magnetic origin and a low cogging torque value, when compared to other conventional concentric winding structures, due to the relatively high Greatest Common Divisor GCD (Q,P) and Least Common Multiple LCM (Q,P) [29]

The studied machine in this paper is a 3-phases electric motor, used in the RENAULT hybrid electric cars (E-Tech System), which the stator magnetic circuit is made with segmented conventional NOES sheets. The main parameters of the motor are presented in Table IV.

The authors study the stator teeth segmentation with GOES sheets, by keeping the geometrical dimensions of the reference motor, as well as the same rotor. The teeth are placed so that the RD is parallel to the radial direction in order to exploit the best performance of the GOES, as shown in Figure 15. This structure allows to minimize the passage of the flux in the GOES difficult magnetisation directions, compared to the structures presented previously as the sheet spatial shifting or the "T-shaped" sectors. Moreover, it is simpler from an industrial point of view compared to the full segmentation of the stator circuit. The teeth width of the motor studied is low so that the effects of the cutting may intervene and considered.

TABLE IV.
MAIN PARAMETERS OF THE STUDIED ELECTRIC MOTOR

Number of Poles / Slots	16 / 24
Winding type	Concentrated
Radius of stator core (outside)	127,5mm
Radius of stator core (inside)	93mm
Airgap (stator - rotor)	0,75mm
Yoke width	11mm
Teeth width	14,5mm
Stator axial length	60,14mm
Stator magnetic material	*25H-EM* (Nippon steel)
Rotor magnetic material	*35H-K375Y* (Nippon steel)
Permanent magnet width	25,5mm
Permanent magnet thickness	4,5mm
Permanent magnet material	*N42SH-R* (Shinitsu)

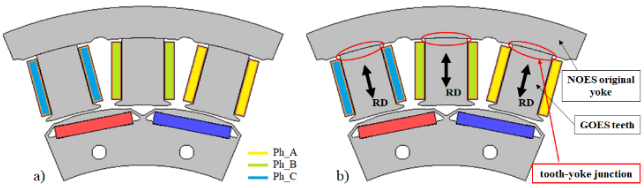

Fig. 15. Stator tooth segmentation: a) NOES reference motor, b) GOES teeth motor

B. Presentation of the experimental model of the phenomena occurring at the tooth-yoke junction

The goal is to investigate the magnetic parameters (flux density and iron losses) depending on the tooth - yoke junction between the two GOES-NOES materials (circled in red in figure 15). Parasitic airgaps at the teeth - yoke junction may also intervene. Thus, several geometries of the junction are proposed according to the ratio / angle of the tooth insertion in the stator yoke.

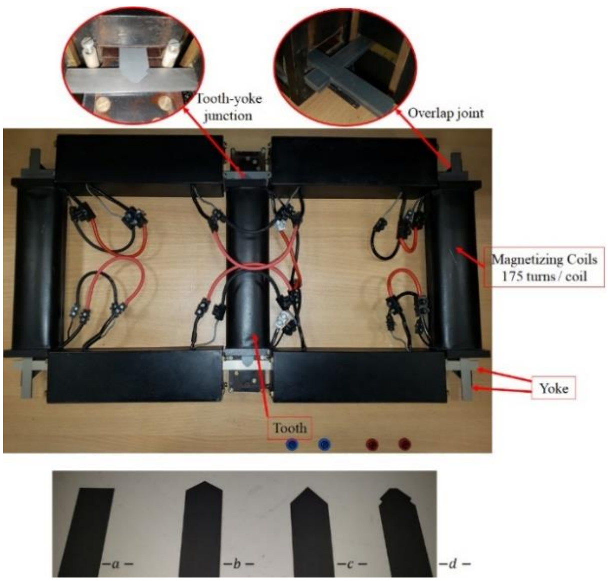

Fig. 16. Experimental device to study the tooth-yoke junction

In order to evaluate the contribution of the elements constituting the magnetic circuit, the device shown in Fig. 16 and 17 is used for both numerical and experimental tests. It combines two modified Epstein frames to magnetize magnetic circuits of different geometries and including junctions. Each arm of the frame is composed of 7 laminations connected with double overlap joints. Weights of 63g are used to hold the joints to minimise the vibration problems. The yoke and the teeth are respectively made of 0.20mm NOES and 0.20mm GOES (reference *PCH20*) from ThyssenKrupp Electrical Steel. The central arm (tooth) is connected to the horizontal limb (yoke) by different kind of junctions. The studied parameters are the angle and the depth of insertion of the teeth into the yoke, as shown in Fig. 17, with 4 different geometries. A particular care is taken to ensure a very low parasitic air gap at the tooth-yoke junction. For the power supply, a voltage sine wave is used.

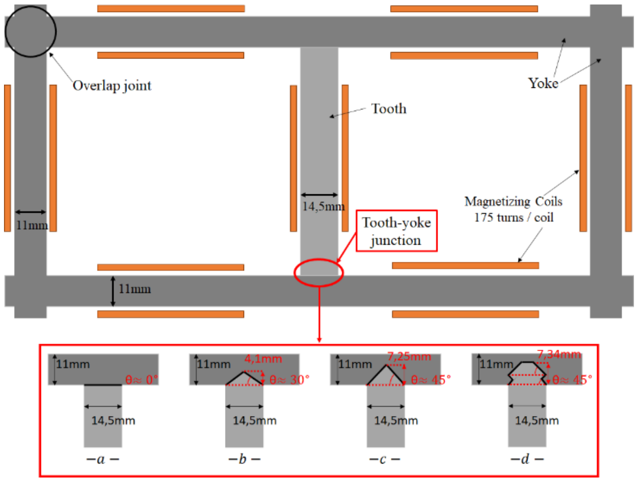

Fig. 17. Details and geometric dimensions of the experimental frame

Then, in concentric winding electrical machines, two main cases can occur depending on the supply:

- the magnetic flux path can be direct from a tooth "N" to teeth "N-1" and "N+1" through the yoke, as shown in Fig. 18-a.
- a tooth may not be solicited so that the flux path goes from a tooth "N" to a tooth N+2", as shown in Fig. 18-b.

In the first case, the central coil, placed in the middle of the frame, is powered. In the second case, the central strips are cut to avoid the flux passing through the central arm and all the lateral coils are powered (see the orange rectangles in figure 18).

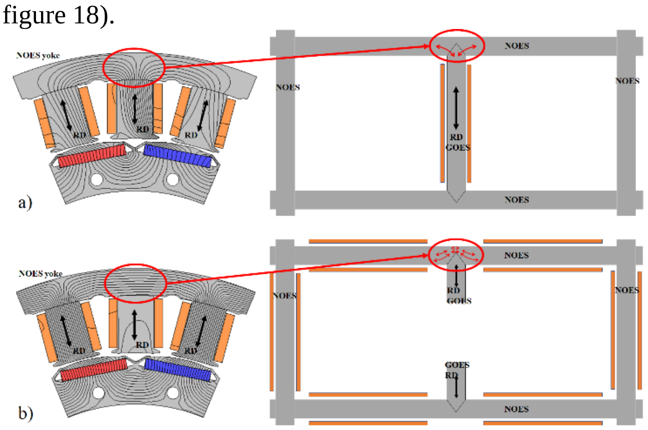

Fig. 18. Phenomena modelled with modified Epstein frames: a) flux passing directly through the teeth, b) flux passing through the yoke

C. Presentation of the iron loss separation method

This section presents how the losses in the magnetic circuit close to the junctions are dissociated from the losses in the corners and the arms. To do that, two frames of different lengths are used and shown in Fig. 19.

Measurements are first made with the frame and the central branch, where the length of the horizontal limbs is 47cm (frame A shown in Fig. 19). Then, measurements are made with a NOES frame for which horizontal limb length is 43.55cm (frame B shown in Fig. 19). The difference in iron losses (equation 4) of these two frames, at iso-frequency and iso-flux density, allows to determine the iron losses in both the central arm and near the tooth-yoke junction. This method is used for the measurements that will be made in the present work

$$P_{tooth-yoke} = P_{frame_A} - P_{frame_B} \quad (4)$$

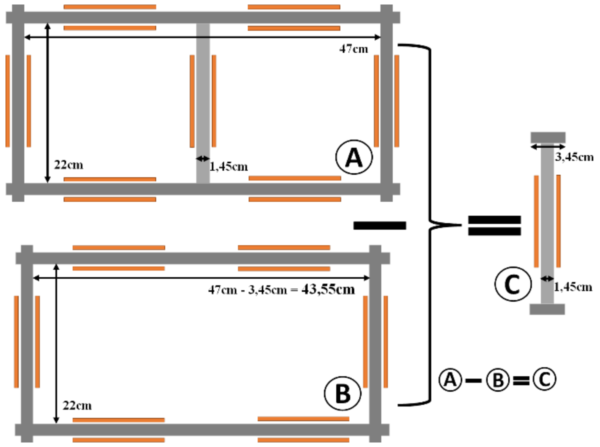

Fig. 19. Experimental method of loss separation

V. Investigation of the tooth-yoke junction in a segmented magnetic circuit

A. Magnetic flux established in the tooth and the yoke

The experimental measurements relative to the first case (path in tooth and yoke) are presented in Fig. 20a and 20b for the different types of tooth-yoke junction. They show the flux density variations as a function of the Ampere-turns (At) and the iron loss variations with B.

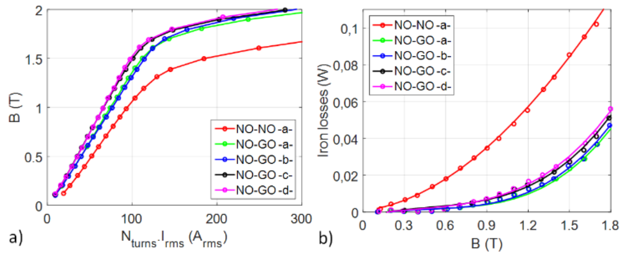

Fig. 20. Experimental results at 50Hz: a) Variation of B with the current, b) Iron loss variations with B

The variation of B with At shows that the use of GOES teeth improves the magnetic circuit permeability, when compared to a full NOES circuit. In addition, the saturation flux density level is improved, around 20% at 200At (Fig 20.a). The mixed circuit allows a strong reduction of iron losses compared to the reference NOES circuit.

For mixed circuit, there are differences in terms of permeability and iron loss depending on the geometric shape of the junction. The strong insertion of the GOES teeth in the yoke (type c and d) gives a better overall circuit permeability. The low insertion leads to lower iron losses. For example, the mixed NOES-GOES structure with no insertion of the teeth in the yoke (type a) has the lowest iron losses, at iso-flux density, compared to other structures. This result is justified by the fact that for geometries b, c and d:

- the flux is not perfectly colinear to the RD near the junction;
- the distribution is not homogeneous at the bottom of the teeth near the junction, leading to more saturated parts.

It is shown in Fig. 22 with the field lines and flux density distribution of the 4 mixed structures at 1.5T and 50Hz.

FEA models introduce a 0.02mm parasitic air gap. Concerning the iron losses, the results obtained at 50Hz and shown in Fig. 21.b follow the same tendencies as the experimental results, with an underestimation at high flux density values and a slight overestimation at low flux density values for the full NOES circuit. The FEA results about the variations of B show similar values for flux density at saturation. In terms of permeability, differences can be seen with the experimental results because the parasitic airgaps are not adjusted, and they have a strong influence as there is no stator – rotor airgap as for a real motor.

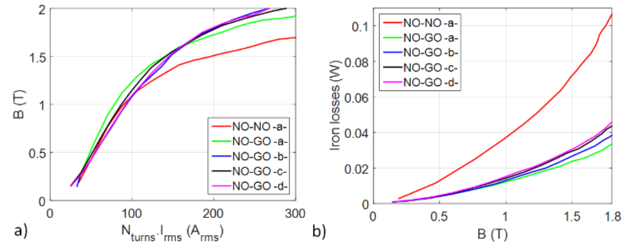

Fig. 21. FEA results at 50Hz: a) Variations of B with the current, b) Iron loss variations with B

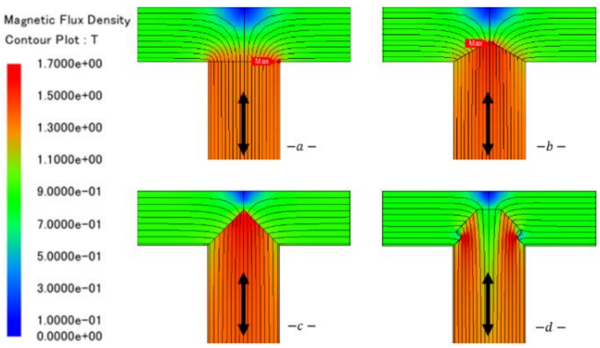

Fig. 22. Magnetic field lines and flux density distribution for the different mixed structures, 1.5T – 50Hz

Considering the frequency variation and the topology -a-, the iron losses of the full NOES circuit are higher than the mixed NOES-GOES circuit, as show in in Fig. 23. For high operating frequencies, differences with experimental results can be explained by the iron loss model taking into account the anisotropy.

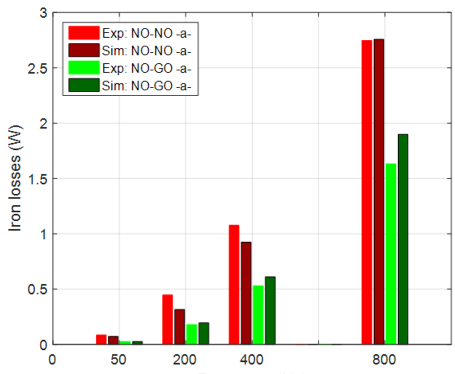

Fig. 23. Comparison of experimental and FEA iron losses with the frequency at 1.5T

From these results, it could be concluded that the -a- type structure is the best assembly in terms of iron losses. However, the non-inserted teeth constitute an ideal case as it is technically difficult to fix the teeth to the yoke and to maintain them because of Maxwell forces applied on them.

B. Effect of the teeth insertion on the yoke

As for the first case, experimental tests and FEA simulations allows to model the passage of the flux only along the NOES yoke. A full NOES circuit with an -a- type junction is used as a reference structure.

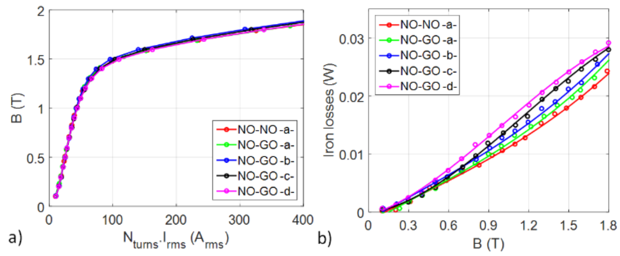

Fig. 24. Experimental results at 50Hz: a) Variation of B with the current, b) Iron loss variations with B

The experimental results, at 50Hz, are presented in figure 24. The differences concerning the variation of B with the current are low; B is slightly higher for structures with low tooth insertion (Fig. 24a). Structures with a strong insertion of the GOES teeth in the NOES yoke have more iron losses because the magnetic flux tends to establish in the NOES more permeable instead of the TD. The distribution of B and the field lines in Fig. 26 for the mixed NOES-GOES junctions show the blockage and the local saturations created by the insertion of the GOES teeth.

As for the first case, the iron losses obtained with FEA (Fig 25.b) have the same variations than experimental results, but with a slight underestimation, especially at low flux density values (below 1T), for all structures.

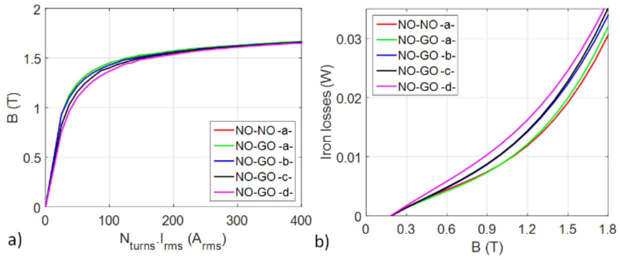

Fig. 25. FEA results at 50Hz: a) Variations of B with the current, b) Iron loss variations with B

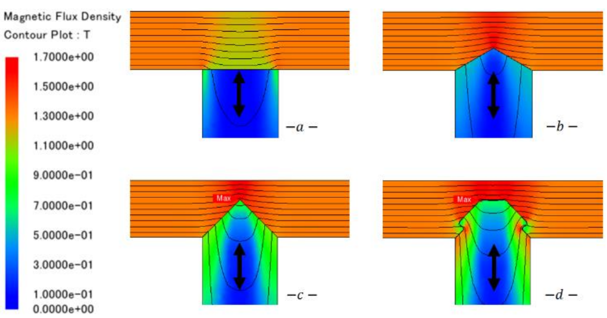

Fig. 26. Magnetic field lines and flux density distribution for the different mixed structures, 1.5T – 50Hz

Considering the frequency influence on iron losses of circuit -a-, FEA and experimental results are close as shown in Fig. 27; there is a slight overestimation of the numerical model.

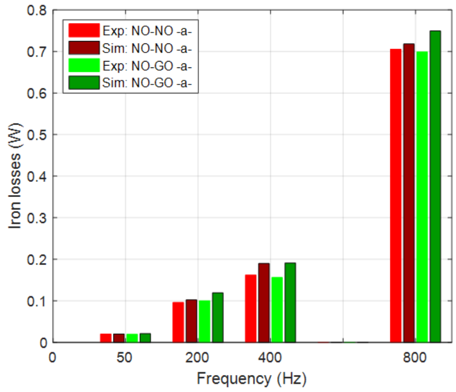

Fig. 27. Comparison of experimental and FEA iron losses with the frequency at 1.5T

VI. Electric Motor Performances with GOES Segmented Teeth

A. Comparison of electromagnetic torque performance

Following the previous results about the iron losses at the tooth-yoke junction, the -a- type junction is considered in the magnetic circuit of the studied motor, keeping the same geometrical dimensions of the NOES reference motor.

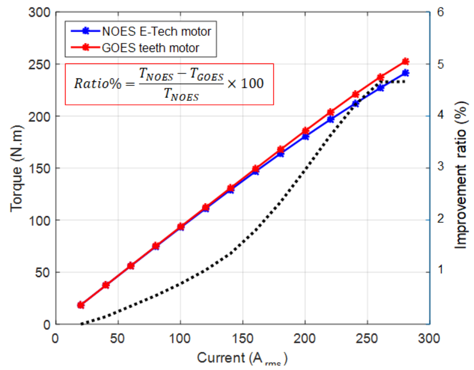

Fig. 28. Current-Torque characteristics at 400Hz [30]

The torque-current characteristics obtained with FEA are presented in Fig. 28 for the two motors. The torque is improved of 4.7% at high load for the mixed steels structure because B is higher for a given current and the use of GOES teeth improves the overall permeability of the circuit, a lower current is needed to magnetize the circuit at a given torque [30]. The flux density distribution, presented in Fig. 29 is quite similar, except around the tips of the magnetized teeth. The distribution in GOES teeth is not homogenous because the flux is mainly driven in the RD. Depending on the position of the rotor, parts of the GOES teeth may be more saturated than for the reference motor [30].

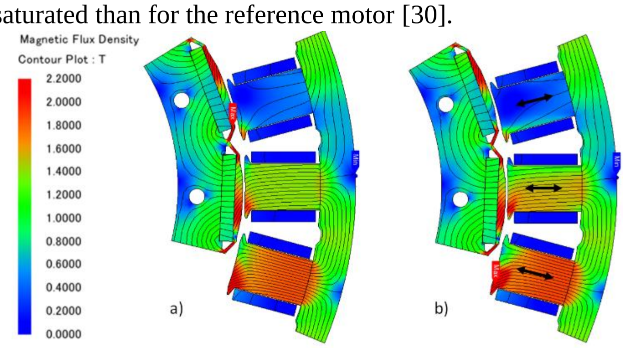

Fig. 29. Magnetic field lines and flux density distribution, at 240N.m - 3000rpm: a) in the NOES reference motor, b) in the GOES teeth motor

B. Comparison of drag losses

The Fig. 30 shows the variation of drag losses in the two motors at different speeds and a significant reduction for the GOES teeth motor. The rate of improvement decreases with speed, from 41% at 500 rpm to 15% at 6000 rpm [30]. The distribution of the drag losses calculated by FEA, at 3000 rpm and over a period, is presented in figure 31. Losses are lower in the GOES teeth. In the stator yoke and the rotor, we notice an identical distribution of iron losses for both motors.

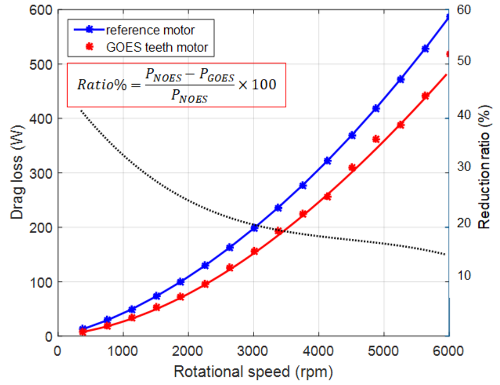

Fig. 30. Drag losses in the reference motor and the GOES teeth motor

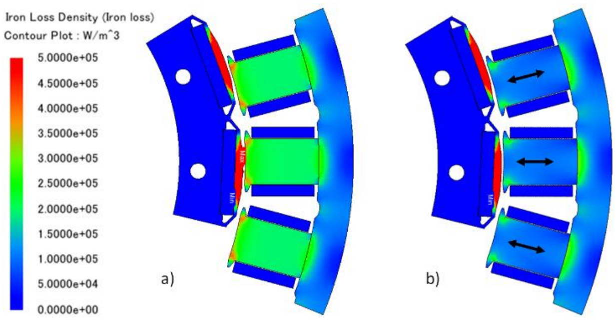

Fig. 31. Drag losses distribution over a period at 3000rpm: a) in the NOES reference motor, b) in the GOES teeth motor

C. Iron losses comparison at iso-torque

Iron losses are calculated for different operating points as a function of load and frequency with more than 400 simulation points for each motor. The loss maps are shown in Fig. 32 and 33 for the two operating modes at steady state: constant torque and flux weakening. Fig. 34 gives the difference ratio at iso-geometry / iso-torque conditions and over the full operating cycle. The gain in iron losses with the GOES teeth structure is highly significant below 4000 rpm and at low load, 42% at very low speeds. At higher speeds, over 4000 rpm, the GOES teeth motor loses its advantage, which can be explained by:

- the strong increase of GOES losses at high frequencies due to the passage of the flux in the hard magnetization direction in the tooth tips [30];
- The two structures have different flux weakening capacities ($Ld_{GOES} \neq Ld_{NOES}$ and $Lq_{GOES} \neq Lq_{NOES}$), which can leads, at an iso-operating point, to a higher flux value for the GOES motor and a lower flux value for the NOES reference motor [30].

This tendency at high frequencies can also be due to the iron losses overestimation with the FEA method taking into consideration the magnetic anisotropy.

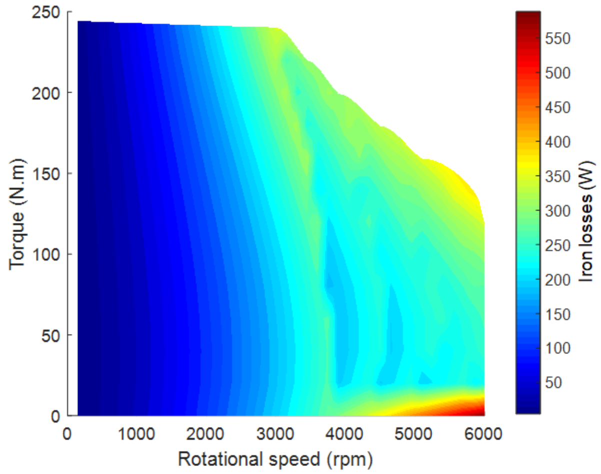

Fig. 32. Iron losses mapping of the NOES reference motor (E-Tech)

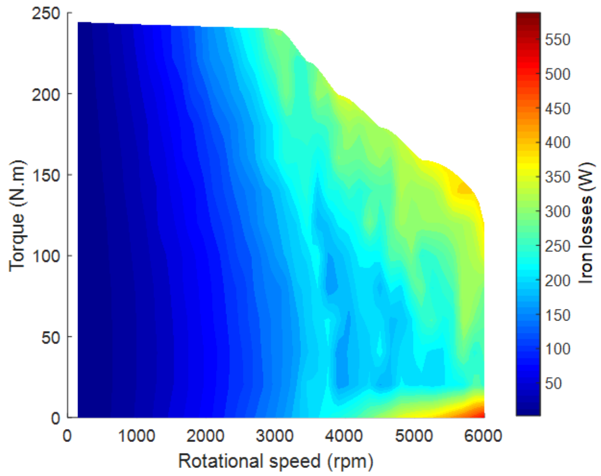

Fig. 33. Iron losses mapping of the GOES teeth motor

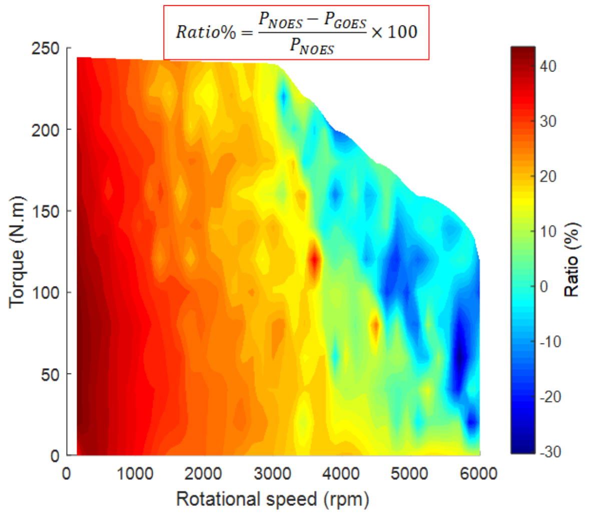

Fig. 34. Difference in iron losses of the NOES reference motor and the GOES teeth motor (reduction - increase ratio)

VII. Conclusion

In this paper, the authors study the potential contribution of the Grain Oriented Electrical Steel mixed with conventional steel in the performance of rotating machine magnetic circuit, with concentred winding. The GOES high anisotropy is an obstacle to their use in rotating field applications, that is why a segmented magnetic circuit is analysed.

To do that, GOES has been firstly characterized and the effect of laser cutting has been analysed. The results show that GOES sheets are highly sensitive to cutting, but they are still more performant compared to conventional NOES sheets. Secondly, a brief panorama shows the existing magnetic circuit made with GOES. Thirdly, the junction between NOES-GOES magnetic materials have been studied by considering several geometrical shapes to choose the best structure in terms of iron losses reduction. An experimental and numerical model was used to reproduce the phenomena existing at the junction. The two main phenomena existing in electric motors with concentric windings were studied. Fourthly, a 24/16 PM motor with GOES sheets has been analysed with FEA calculations. The results show that the use of GOES teeth leads to a significant improvement in torque at high loads. In terms of iron losses, the mixed NOES-GOES stator circuit allows a significant drag loss reduction, especially at low operating speeds, where the reduction ratio is more than 41%. For the iron losses over the whole operating range of the electric motor, a high reduction is observed for speeds below 4000rpm with the GOES teeth motor. For higher speeds, the reduction ratio of iron losses is not so important.

ACKNOWLEDGMENT

The authors thank thyssenkrupp Electrical Steel (TKES UGO, Isbergues - France) for providing the GOES laminations.

REFERENCES

[1] D. Auverlot, N. Meilhan, B. Mesqui et A. Pommeret, Les politiques publiques en faveur des véhicules à très faibles émissions, France: France stratégie, 2018.

[2] J.Pyrhonen, T.Jokinen et V.Hrabovcova, Design of Rotating Electrical Machines (Seconde Edition), Wiley, 2014.

[3] K. Fujisaki, Magnetic Material for Motor Drive Systems, Singapore: Springer, 2019.

[4] N. Soda et M. Enokizono, «Improvement of T-Joint Part Constructions in Three-Phase Transformer Cores by Using Direct Loss Analysis with E&S Model,» *IEEE, TRANSACTIONS ON MAGNETICS*, vol. 36, n°14, pp. 1285 - 1288, 2000.

[5] K. Fujisaki et K. Fujitani, «Design of stator core shape of magnetic anisotropic motor,» *IEEE, International conference on electrical machines*, pp. 183 - 189, 2012.

[6] E. G. Araujo, J. Schneider, K. Verbeken, G. Pasquarella et Y. Houbaert, «Dimensional effects on magnetic properties of FE-Si steels due to laser and mechanical cutting,» *IEEE*, pp. 213 - 216, 2010.

[7] P. K. Klimczyk, P. Anderson, A. Moses et M. Davies, «Influence of Cutting Techniques on Magnetostriction Under Stress of Grain Oriented Electrical Steel,» *IEEE, TRANSACTIONS ON MAGNETICS*, vol. 48, n°14, pp. 1417 - 1420, 2012.

[8] A. Jansen, «Grain oriented electrical steel for energy efficient transformers,» ThyssenKrupp, Gelsenkirchen, 2013.

[9] R. Sundaria, A. Daem, A. Hemeida, P. Sergeant, A. Arkkio et A. Belahcen, «Effect of Different Cutting Techniques on Magnetic Properties of Grain Oriented Steel Sheets and Axial Flux Machines,» *IEEE, annual conference of the IEEE industrial electronics society*, pp. 1022 - 1027, 2019.

[10] T. Tamaki, K. Fujisaki, K. Wajima et K. Fujiwara, «Comparison of Magnetic Field Analysis Methods Considering Magnetic Anisotropy,» *IEEE TRANSACTIONS ON MAGNETICS*, vol. 46, n°12, pp. 187 - 190, 2010.

[11] T.Nakata, K.Fujiwara, N.Takahashi, M.Nakano et N.Okamoto, «An Improved Numerical Analysis of Flux Distributions in Anisotropic Materials,» *IEEE Transaction on magnetics*, vol. 30, n°15, pp. 3395 - 3398, 1994.

[12] A. di Napoli and R.Paggi, «A model of anisotropic grainoriented steel,» *IEEE Trans. Magnetics*, 1983.

[13] F. Jiang, M. Rossi et G. Parent, «Anisotropy model for modern grain oriented electrical steel based on orientation distribution function,» *AIP Advances*, vol. 8, n°1056104, 2018.

[14] J. Liu, A. Basak, A. J. Moses et G. H. Shirkoohi, «A Method of Anisotropic Steel Modelling Using Finite Element Method with Confirmation by Experimental Results,» *IEEE TRANSACTIONS ON MAGNETICS*, vol. 30, n°15, pp. 3391 - 3394, 1994.

[15] D. Lin, P. Zhou, Z. Badics, W. N. Fu, Q. M. Chen et Z. J. Cendes, «A New Nonlinear Anisotropic Model for Soft Magnetic Materials,» *IEEE TRANSACTIONS ON MAGNETICS*, vol. 42, n°14, pp. 963 - 966, 2006.

[16] A. Krings et J. Soulard, «OVERVIEW AND COMPARISON OF IRON LOSS MODELS FOR ELECTRICAL MACHINES,» *Journal of Electrical Engineering*, p. Mai, 2010.

[17] D. Kowal, P. Sergeant, L. Dupré et A. V. D. Bossche, «Comparison of Nonoriented and Grain-Oriented Material in an Axial Flux,» *IEEE, transiction on magnetics*, vol. 46, n°12, pp. 279 - 285, 2010.

[18] Y. YU, Y. Bi, Z. Hao et Y. Pei, «Performance analysis between Grain-oriented and Non-oriented Material on Yokeless And Segmented Armature Machine,» *IEEE, international conference on electrical machines and systems*, 2019.

[19] K. Akatsu et Y. Sugawara, «Characteristics of a SRM using GO electrical steel,» *IEEE, International conference on electrical machines & systems*, pp. 1105 - 1110, 2013.

[20] S. Lopez, B. Cassoret, J.-F. Brudny, L. Lefebvre et J. N. Vincent, «GO steel assembly characterization for the developement of high effeciency AC rotating electrical machines,» *IEEE, Transaction on magnetics*, pp. 4161 - 4164, 2009.

[21] V. Mallard, C. Demian, J.-F. Brudny et G. Parent, «The use of segmented-shifted grain-oriented sheets in magnetic circuits of small AC motors,» *Open Physics*, vol. 17, pp. 617 - 622, 2019.

[22] J. W. Apperson et C. B. Fontaine, «The Use of Preferred Orientation Strip Steel in Turbine-Generator Stator,» *IEEE (AIEE Transactions)*, pp. 836 - 840, 1951.

[23] T. Tomida, N. Sano, S. Hinotani, K. Fujiwara, H. Kotera, N. Nishiyama et Y. Ikkai, «Application of fine-grained doubly oriented electrical steel to IPM Synchronous motor,» *IEEE, Transactions on Magnetics*, vol. 41, n°110, pp. 4063 - 4065, 2005.

[24] R. Pei, L. Zeng, S. Li et T. Coombs, «Studies on GO silicon steel used in traction motor,» *IEEE, International conference on electrical machines & systems*, 2017.

[25] E. A. Périgo et D. Tremelling, «Grain oriented particles for energy applications,» *IEEE, Magnetics letters*, vol. 9, 2018.

[26] P. Pillay et S. Taghavi, «An innovative rotor core assembly for high performance 4 pole synchronous reluctance traction motor using GO lamination,» *IEEE, International electrical machines & drives confrence*, pp. 90 - 95, 2015.

[27] S. Takeda, K. Fujitani, S. Odawara et K. Fujisaki, «Trial manufacture of magnetic anisotropic motor and evaluation of drag loss characteristics,» *IEEE, International conference on electrical machines*, pp. 2055 - 2061, 2014.

[28] N. Denis, S. Takeda, K. Fujitani, K. Fujisaki et S. Odawara, «Anisotropic magnetic core for the iron loss reduction of permanant magnet synchronous motor,» *Journal of the magnetics society of Japan*, vol. 42, p. 62 - 71, 2018.

[29] M. Farshadnia, Advanced Theory of Fractional-Slot Concentrated-Wound Permanent Magnet Synchronous Machines, Singapore: Springer Nature, 2018.

[30] A. Rebhaoui, S-A. Randi, C. Demian et J-P. Lecointe, «Using Grain Oriented Electrical Steel Sheets for Electric Motor in Automotive Application: Tooth Segmentation,» *20th International Symposium on Electromagnetic Field*. Lodz/Cracow, Poland, September 2021.